POLITECNICO DI TORINO
Repository ISTITUZIONALE

Instability assessment of shallow structures using image capturing

Original
Instability assessment of shallow structures using image capturing / Bazzucchi, Fabio; MANUELLO BERTETTO, AMEDEO DOMENICO BERNARDO; Carpinteri, Alberto. - ELETTRONICO. - (2017). (Intervento presentato al convegno INTERFACES - architecture, engineering, science - IASS 2017 tenutosi a Hamburg nel September 25th - 28th, 2017).

Availability:
This version is available at: 11583/2683525 since: 2017-10-01T13:16:57Z

Publisher:
HafenCity University Hamburg & International Association of Shell & Spatial Structures

Published
DOI:

Terms of use:
openAccess

This article is made available under terms and conditions as specified in the corresponding bibliographic description in the repository

Publisher copyright

(Article begins on next page)

05 May 2023

September 25th - 28th, 2017
INTERFACES
architecture . engineering . science IASS 2017 hamburg

Proceedings of the IASS Annual Symposium 2017
"Interfaces: architecture.engineering.science"
September25 - 28th, 2017, Hamburg, Germany
Annette Bögle, Manfred Grohmann (eds.)

Instability assessment of a shallow structure through image capturing

Fabio BAZZUCCHI*, Amedeo MANUELLO[a], Alberto CARPINTERI[a]

*Politecnico di Torino - Department of Structural, Geotechnical and Building Engineering
Corso Duca degli Abruzzi, 24, 10129, Torino, IT
fabio.bazzucchi@polito.it

[a]Politecnico di Torino - Department of Structural, Geotechnical and Building Engineering

Abstract

Recent studies regarding the buckling vs snap-through interaction for imperfect shallow structures, have shown that, after the nonlinear bifurcation, load reductions occur accompanied with a predictable tendency [1,2]. To obtain this behavior, *interaction domains* and *curves,* reported in Bazzucchi et al [2], have been theoretically and numerically defined. In this paper, various steel Von Mises truss-like were built, tested and numerically analyzed through geometrically nonlinear analysis (GNIA). Every structural arrangement was analyzed with regards to different shallowness ratios, slenderness, restraining conditions and imperfection patterns. It was observed how these driving parameters could be interpreted by two original interaction (Δ) and form (Ω) factors.

At the same time, these factors were evaluated for each assembled model through an image processing algorithm. At the end, experimental interaction domains were traced and compared to the numerical ones. Results showed good agreement with the theoretical and numerical expected outcomes. In the Authors opinion, this approach could be promisingly applied for the passive stability assessment of shallow structures.

Keywords: snap-through, buckling interaction, geometric nonlinearity, imperfection pattern, image capturing, interaction domains.

1. Introduction

In plane buckling of shallow arches is a traditional problem in structural engineering [3,4]. Although it has been long investigated, the topic continues to fascinate the research community due to its fundamental relevance for the stability of reticulated structures [5,6,7,8], for the mechanical assessment of buckling-induced smart applications [9,10] and for the stability of material lattices [11]. Even if it is treated in *static* way, the problem has an intrinsic dynamic nature that makes necessary the use of refined numerical methods. Closed-form solutions exist only for particular configurations and their effectiveness stays for reference and comparisons [12,13]. Moreover, the imperfection sensitivity of the systems implicates the adoption of some expedients to take into account their unknown entity. Usually this is resolved by combining a set of the buckling eigenvalues or by a probabilistic approach. In the former case, a minimum computational commitment is required but a conclusive criteria about the eigenvalue selection does not exists [14]. In the latter case, to achieve a robust safety factor, a very high number of analysis must be performed [15].

From a numerical point of view, the most common solution scheme adopted is a geometrically nonlinear analysis with imperfections included (GNIA). Equilibrium equations must be written in a follower reference system and the arc-length control is necessary to overpass the limit point that coincide with the snap-through load [16]. The use of displacement control allows the exclusion of the

Copyright © 2017 by Fabio Bazzucchi, Amedeo Manuello and Alberto Carpinteri
Published by the International Association for Shell and Spatial Structures (IASS) with permission.

arc-length control scheme but the limit points must be priory defined by a bracketing algorithm [2]. In such circumstances (especially for SDOF systems), the nonlinear displacement field has to be obtained step-by-step then is necessary a deep investigation of the mechanical behavior of the structure. In order to do it, the tool of the interaction domains represents an effective solution to located the weakest part and the local failures. When all these conditions are satisfied, the described method is the fastest way for an instability assessment.

In the present paper, an original method is proposed for a simple structure, based on the described above procedure. The preliminary identification of the defected shape is performed by a novel algorithm using digital image processing. These first outputs allow to estimate the ultimate load towards vertical load instability. The proposed method has been validated by the experimental evidences and the analytical calculation of a reduction load function *R*.

2. Form and interaction factors

For geometrically nonlinear structures, instability generally occurs by a snap-buckling. However, the local (or global) buckling of the structure can interact with the snap-through instability, generating the so-called *coupled instability* or *interactive buckling*. Its existence is determined by the relation between the shallowness ratio (*h/d*) and the slenderness (λ) of the structure. For a Von Mises truss (Fig. 1a), this relation appears as a closed-form curve, called *interaction curve* that separates in the λ-*h/d* plane the structural configuration affected by a coupled instability by the one affected by the sole snap-through (Fig. 1a). Taking into account the presence of imperfections (i.e. midspan deviations from the line axis of the bars), an interaction domain like the one reported in Fig. 1.b can be built. From this tool the buckling load reduction (with respect to the perfect system instability load $\boldsymbol{F_{PERF}}$) associated to a certain imperfection can be predicted. Its construction pass through the displacement control GNIA analyses described in the previous Section.

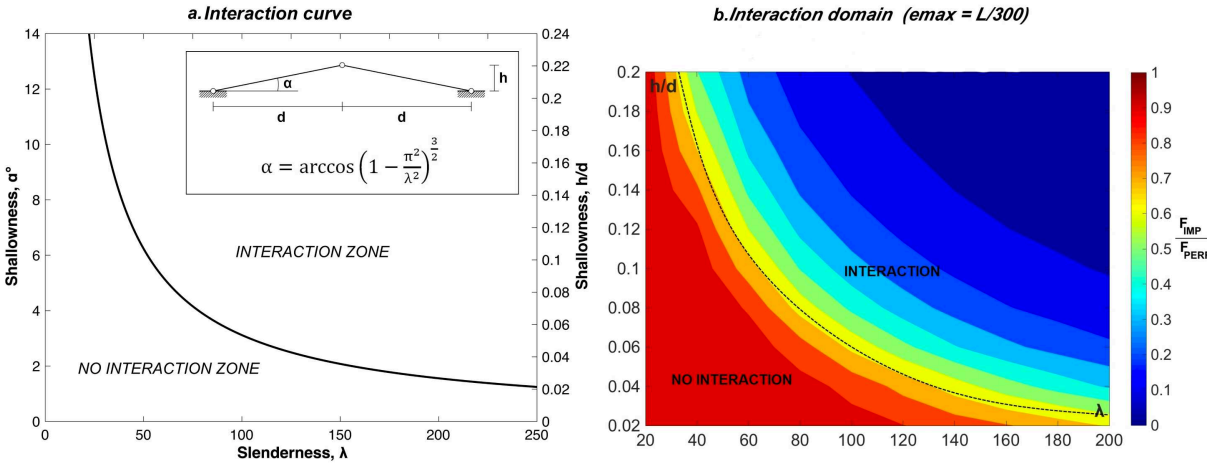

Figure 1: a. the interaction curve for the Von Mises truss; b. interaction domain built for a midspan deviation equal to 1/300 of the bar length.

When the system in Fig. 1a is clamped instead of hinged, the shape of the imperfection becomes relevant since it determines the interactive buckling branch. The Authors [17] demonstrated that the load reduction occurs with a predictable tendency, when the correlation between existing imperfections and buckling eigenshapes passes through a form factor Ω. This index works differently from the classic similarity eigenvalue indexes like MAC because it is able to take into account the asymmetric configurations without the sign classification. In detail, it accounts on a fundamental parameter Δ, that indicates the vertical distance between the midspan deviations (Fig. 2a). Applying a

random set of imperfection patterns to the system in Fig. 1a, it is possible to observe that the equilibrium paths follow a decreasing trend as Δ increases (Fig. 2d). As an example, for the left bar, The factor Δ_{sx} can be easily derived from the midspan deviation $e_{0,sx}$ by the following relation

$$\Delta_{sx} = e_{0,sx}\sqrt{1+\left(\frac{h}{d}\right)^2} \tag{1}$$

as indicated in Fig. 2c. Then, complete Δ factor can be easily obtained by adding Δ_{sx} and Δ_{dx}. Δ, defined as interaction factor, is able to maximize the similarity between a pre-deformed shape and the first buckling eigenvalue (this can be demonstrated by evaluating a typical similarity index for image correlation as the second order Minkowski metric). Including Δ into a more general *form factor* Ω, formulated as:

$$\Omega = \beta^2\left[\frac{\Delta}{s}+\left(\frac{e_{max}}{s}\right)^2\right] \tag{2}$$

the restraining conditions and the geometric configuration can be taken care by a single parameter.

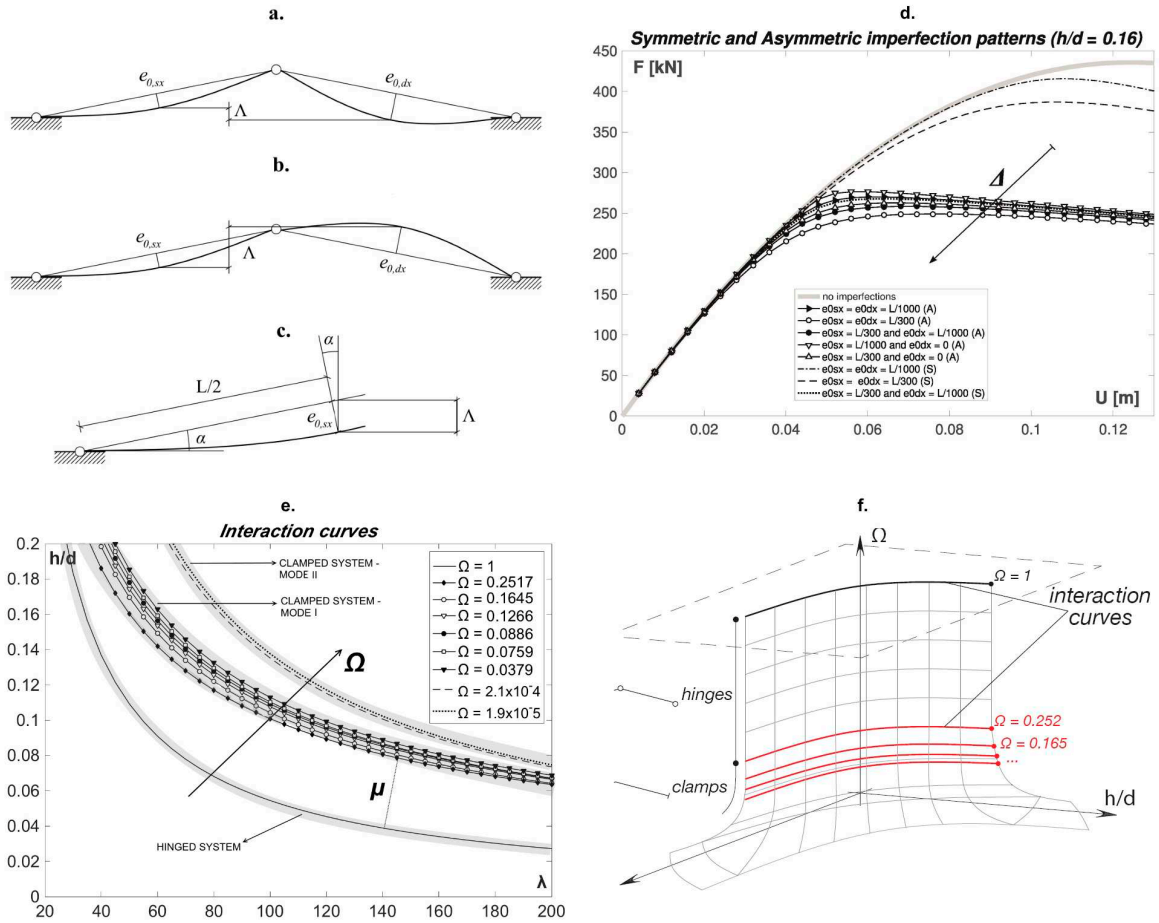

Figure 2: a,b,c. Δ parameter for the Von Mises truss; d. equilibrium paths with the imperfection patterns applied; e. interaction curves; f. interaction surface.

In fact, β represents the multiplier of the free length of the single constituting bar, S is the span get involved in the buckling eigenshape and e_{max} is the maximum applied deviation. Operating this way, not only the equilibrium paths, but also the interaction curves can be ordered in a predictable trend (Fig. 2d). Each curve can be catalogued by μ, which is a function of the slenderness and the shallowness ration, of the generic interaction curve from the fundamental one (related to the hinged perfect system). It is possible to demonstrate [17] that all the possible interaction curves (i.e. every imperfection pattern) belong to a ramp surface (Fig. 2e) that can be obtained by a 3D polynomial interpolation law with the following form:

$$\frac{h}{d} = a\lambda^{-b} \tag{3}$$

where a and b are parameters that can be obtained by selecting a minimum number of 4 interaction curves. Working out on these parameters, a load reduction function $R(\Omega,\mu)$ can be extracted and, for a chosen imperfection pattern it gives back the load reduction factor to apply to the perfect system instability load $\boldsymbol{F_{PERF,}}$ in order to obtain the actual critic instability load of the system $\boldsymbol{F_{cr}}$:

$$Fcr = RF_{PERF}. \tag{4}$$

Because of its nature, R coincides with the ratio mapped on the relative interaction domain, but with a consistent reduction on the computing commitment: R can be computed just by 4 random imperfection patterns. This means that, knowing the geometry of the structure, its material and inertial properties, and the imperfection applied a fast assessment of the maximum instability load can be outperformed by (4). In the next Section, the application of this method will be shown together with a photography based structural identification.

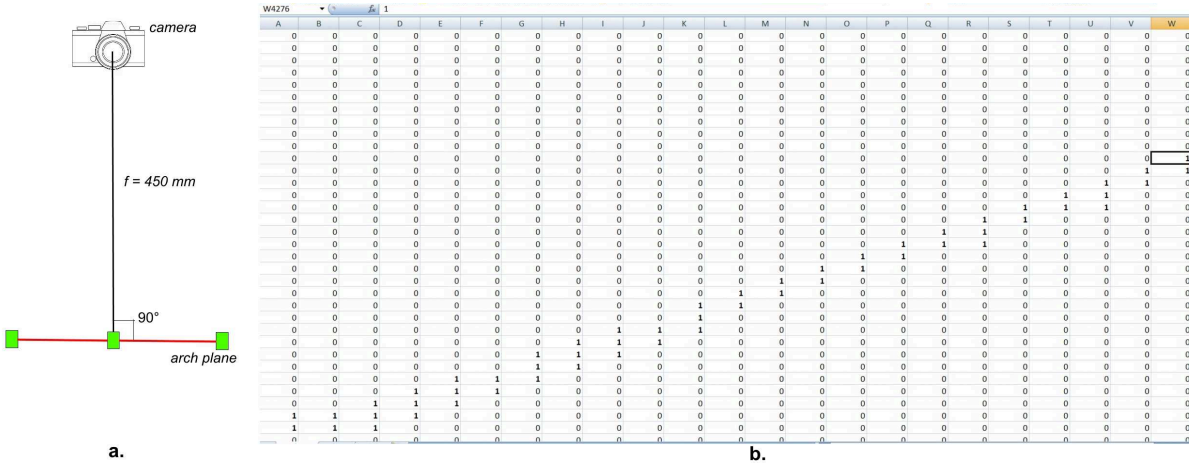

Fig. 3: a. arrangement of the image capturing system; b. the identified structure, transformed in a binarized matrix (plotted on Excel).

3. The recognition algorithm

The structural identification of the Von Mises arch from a digital photography was carried out by a custom algorithm base on the digital image processing of the image of the structure. Since the considered imperfections have the order of magnitude of the 10^{-1} mm, the captured image necessitated a resolution in the order of 10^{-2} mm. In order to do so, the image capturing apparatus provided for a RAW images with a resolution of 6016×4016 pixels at 300 ppi. The distance of the camera from the arch was fixed in 450 mm (Fig 3a), then providing to the algorithm known distance (i.e. the bar length), the geometrical identification of the arrangement could be performed. In detail, for each of the Von Mises arches that have been tested, 50 images have been taken with a rapid sequence in the undisturbed state of the arch. The digital image processing, carried out by a Phyton code, consists in

two phases (i) binarizing and (ii) filtering [18]. In the first step, the algorithm selecting all the red and green RGB pixel (with a tolerance of ± 25). These two colors were in fact used to manufacture the bars and the constraint respectively (Fig. 4). Once the image was binarized, the filtering procedure to eliminate the eventual residual digital noise around the arch was applied. Applying those procedures to every picture taken and considering the average values the photography identification was complete. The resultant image, contains a b/n picture that could be written in a matrix form that contains the x-y coordinate of each point (Fig. 3b). By these coordinates, the midspan deviation can be identified, together with the geometrical characteristics of the arch. As a consequence, the Ω factor can be immediately identified.

4. Experimental set-up

The experimental set-up of the tests was constituted by a set of aluminum bars with a cross-section of 2 × 10 mm. The bars were connected by wood elements able to reproduce the clamp constraint condition. The node disposed in the middle of the structure was realized by a cylindrical element with two incisions made with a carving inclination of 10 degrees. The two extreme joints were realized by semi-cylindrical elements with the same carving notch. The Von Mises arch, performed experimentally, was fixed on the work bench at a defined distance in order to obtain a prescribed shallowness ratio equal to 0.17. In Fig. 4a the structure is observed from a lateral point of view. Before to start the tests both the correct rectilinear configuration and the shallowness ratio were checked. In Fig. 4b and c the frontal and the perspective view of the tested structure are reported. In the present paper, in particular, two different length of the mid-span were considered during the experimental campaign: 295 mm and 245 mm. the length of the bars used are 300 mm and 250 mm respectively. The imperfections as geometrical defects were imposed on the bars by means of weight concentrated just in the middle of the two elements. The adopted load of 95 g and 135 g were applied using cables fixed in the middle of each portion of the arch, as reported in Fig. 4c. The two load levels were used to obtain a prescribed mid-span deviation. These loads did not affected the measurements considering that they were irrelevant respect to the ultimate load level and their vibration is far from the oscillating configuration of the whole structure around the deformed shape. The inflexions provoked were ranging between 1/250 and 1/280 of the bar length for both the two bar types. On the other hand, the increasing load used to carry out the test, was applied on the central node (cylindrical connection). The application of the force has been effectuated gradually imposing a step by step increment of about 50 g up to the peak load. As reported in Fig. 4, the work bench was carved in order to apply the load and to allow the non adjacent configuration of the equilibrium after the snap-through of the arch. In Tab 2 the geometrical characteristics of the arches and the geometrical defect obtained by the load application were summarized.

Table 1: Experimental set-up: Geometrical configurations and geometrical defect load application

Length of each bar (mm) [L]	**Mid-span arch (mm) [*d*]**	**Load for geometrical deviation (g)**
300	295	95
250	245	135

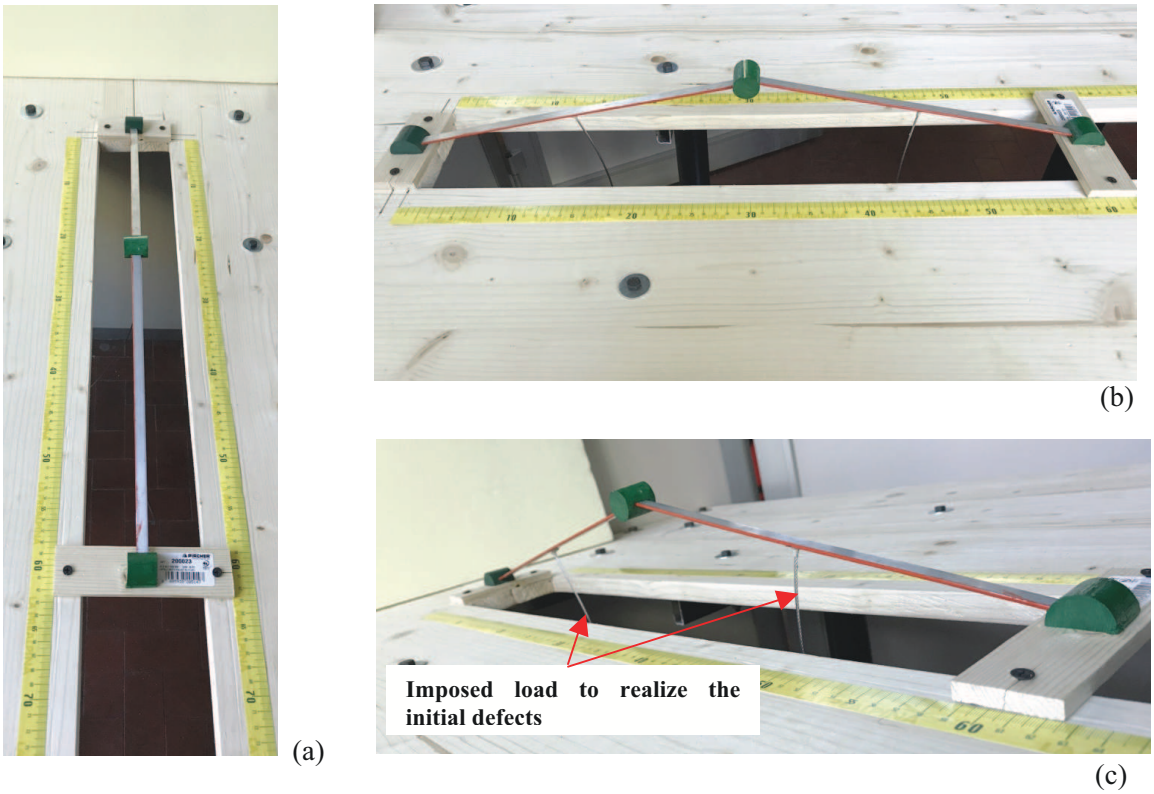

Fig. 4: Lateral (a), frontal (b) and perspective (c) view of one of the structures adopted during the experimental campaign.

5. Results

In Figure 5, the identified structures were reported with an increasing number that indicates the test number. Results from test 2, reported a failure load (associated with a snap-through phenomenon) of 1450 g, indicating a reduction from the buckling expected load (F_{PERF} = 33.2 N) of the 56.3%. Results of the all conducted tests were reported in Table 2.

Table 2: Comparison between tests and expected buckling load.

Test number	Buckling load (test) [N]	Buckling load (computed) [N]	Load reduction [%]
1	18.75	33.2	43.5
2	14.50	33.2	56.3
3	28.0	40.5	30.9
4	19.50	40.5	51.85

In order to evaluate the function *R*, the interaction curve of the system must be obtained. In order to do so, the reference [17] were used, which collect a series of interaction curves and domains for the Von Mises Arch-like structures. The corresponding Ω factors of each structure, identified by the image capturing algorithm, were reported in Table 3, together with the *R* function, computed by a literature

reference of μ. It is possible to observe that the variation from the experimental loads differenced from the digital photography assessment by a maximum value of 6.8 %.

Table 3: Comparison between tests and expected buckling load.

Test number	Ω	μ (normalized)	R
1	0.0095	1	0.65
2	0.0180	0.56	0.41
3	0.0053	0.74	0.68
4	0.0089	0.95	0.47

Finally, the bifurcation branches of the arches were reported in Fig. 6 together with the experimental loads obtained and the one computed by digital identification. Moreover, one of the equilibrium path computed by GNIA of the test 3 was overlapped in Fig 6. It can be noticed that the limit point lays in the zone detected by the experimental tests and the fast formula (4).

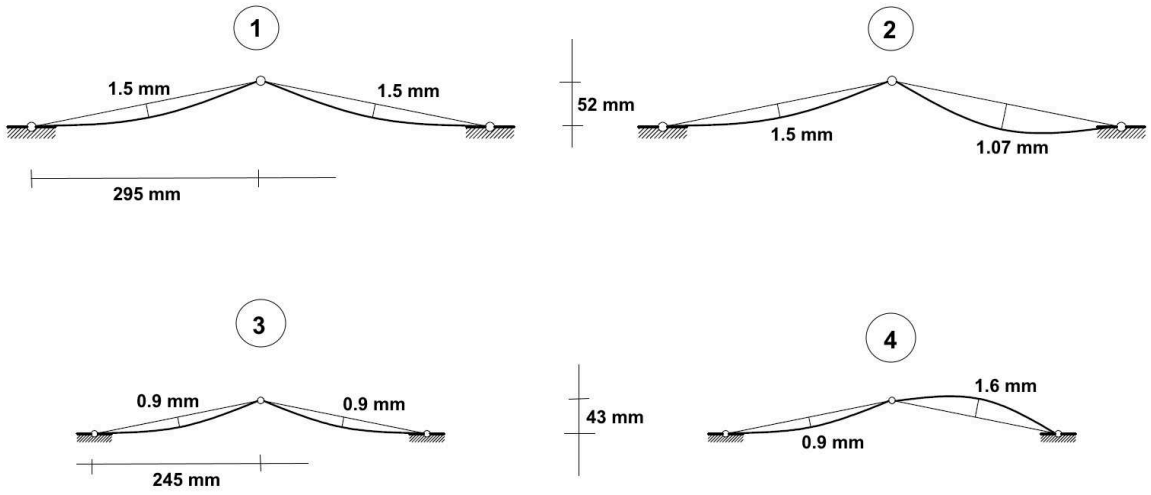

Fig. 5: Identified and tested stuctures.

6. Conclusions

In this paper, the possibility to assess the instability load of a system through image capturing was presented. Several Von Mises arch-like structure were realized, tested and identified by photo capturing.

Through digital processing of the captures images of the structures, two fundamental indexes have been evaluated. They have been correlated with reference values based on the interaction analyses between buckling and snap-through. A load reduction function has been extracted and the expected buckling load has been estimated.

The load testing has been carried out through a step-by-step system with an increasing force of 0.005N. 4 Von Mises arches have been tested, constituting in alloy bars of length 300 and 250 mm. The shallowness ratio has been fixed in 0.17 and a random imperfection pattern has been applied to each tested arrangement.

It has been possible to observe that the variation from the experimental loads differences from the digital photography assessment by a maximum value of 6.8 %. At the same time, the GNIA analysis of one of the identified configuration showed that the limit point is consistent with the obtained results.

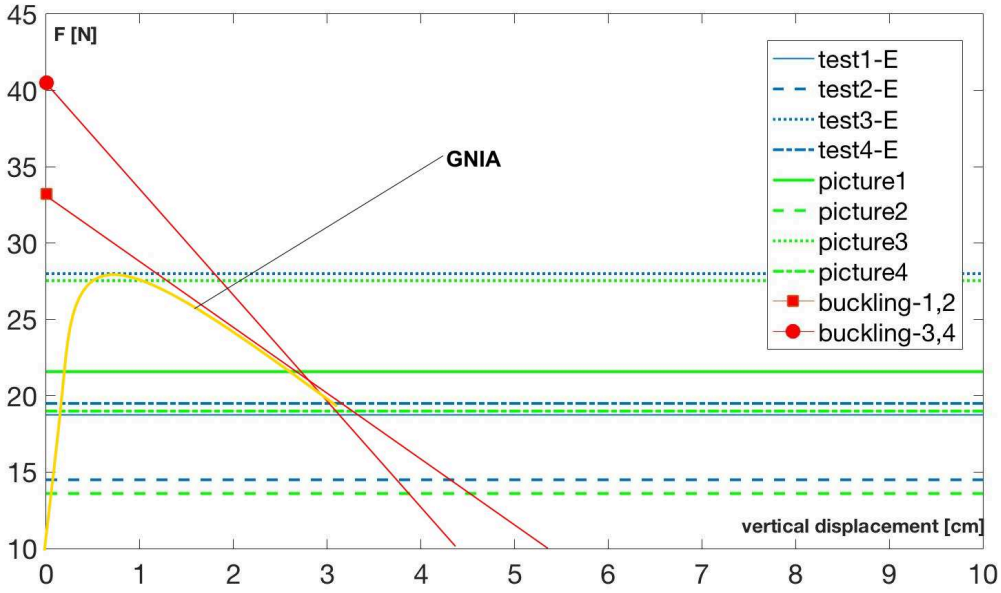

Fig. 6: Load comparison and equilibrium paths.

References

[1] Pecknold, D. A., J. Ghaboussi, and T. J. Healey. Snap-through and bifurcation in a simple structure. *Journal of Engineering Mechanics*,1985; **111.7**; 909-922.

[2] Bazzucchi, F., A. Manuello, and A. Carpinteri. Interaction between snap-through and Eulerian instability in shallow structures. *International Journal of Non-Linear Mechanics*,2017; **88**; 11-20.

[3] Timoshenko, S., 1970. *Theory of Elastic Stability 2e*. Tata McGraw-Hill Education.

[4] Pi YL, Trahair NS. In-plane buckling and design of steel arches. *Journal of Structural Engineering*,1999;**125(11);**1291-8.

[5] Shen, S.Z. and Chen, X., Stability of reticulated shells. *Science Press, Beijing, China*, 1999;122-158.

[6] Fan, F., Cao, Z. and Shen, S., Elasto-plastic stability of single-layer reticulated shells. *Thin-Walled Structures*, 2010;**48**(10);827-836.

[7] Gioncu, V., Buckling of reticulated shells: state-of-the-art. *International Journal of Space Structures*, 1995;**10**(1);1-46.

[8] Bazzucchi F., Carpinteri A., Manuello A., Interaction between different instability phenomena in shallow roofing structures affected by geometrical imperfection in *IASS 2016. Spatial Structures in the 21st Century*, Ken'ichi Kawaguchi, Makoto Ohsaki, Toru Takeuchi (ed.), CEDEX Madrid, Spain, 2016.

[9] Hu, N. and Burgueño, R., Buckling-induced smart applications: recent advances and trends. *Smart Materials and Structures*, 2015;**24**(6);063-001.

[10] Virgin, L.N., Guan, Y. and Plaut, R.H., On the geometric conditions for multiple stable equilibria in clamped arches. *International Journal of Non-Linear Mechanics*, 2017;**92**;8-14.

[11] Danso, L.A. and Karpov, E.G., Cusp singularity-based bistability criterion for geometrically nonlinear structures. *Extreme Mechanics Letters*, 2017,in press

[12] Bradford, M.A., Uy, B. and Pi, Y.L., In-plane elastic stability of arches under a central concentrated load. *Journal of engineering mechanics*, 2002;**128**(7);710-719.

[13] Pi, Y.L., Bradford, M.A. and Tin-Loi, F., Nonlinear analysis and buckling of elastically supported circular shallow arches. *International Journal of Solids and Structures*, 2007;**44**(7);2401-2425.

[14] Touzé, C., Vidrascu, M. and Chapelle, D., Direct finite element computation of non-linear modal coupling coefficients for reduced-order shell models. *Computational Mechanics*, 2014;**54**(2);567-580.

[15] Yan, J., Qin, F., Cao, Z., Fan, F. and Mo, Y.L., Mechanism of coupled instability of single-layer reticulated domes. *Engineering Structures*, 2016;**114**;158-170.

[16] Crisfield, M.A., A fast incremental/iterative solution procedure that handles "snap-through". *Computers & Structures*, 1981;**13**(1-3);55-62.

[17] Bazzucchi, F., Shallow-dome structures and interaction between buckling and snap-though. Politecnico di Torino, 2017.

[18] Garcia-Sucerquia, J., Ramírez, J.A.H. and Prieto, D.V., Reduction of speckle noise in digital holography by using digital image processing. *Optik-International Journal for Light and Electron Optics*, 2005;**116**(1);44-48.